

**Supporting Information For:**

**A Functionalized Hf(IV)–Organic Framework Introducing Efficient, Recyclable and Size Selective Heterogeneous Catalyst on MPV Reduction**

*Aniruddha Das*<sup>\*a</sup>, *Asit Kumar Das*<sup>\*b</sup>

<sup>a</sup>Analytical and Environmental Science Division and Centralized Instrument Facility, CSIR-Central Salt and Marine Chemicals Research Institute, Bhavnagar, Gujarat 364002, India.

<sup>b</sup>Department of Chemistry, Krishnath College, Berhampore, Murshidabad, West Bengal, 742101, India.

\*Corresponding author. Tel: +91-9706675521; +91-7001013825

E-mail address: [dasaniruddha1991@gmail.com](mailto:dasaniruddha1991@gmail.com); [akdas.chem@gmail.com](mailto:akdas.chem@gmail.com)

**Materials:** All the chemicals such as Hafnium tetrachloride, 2-aminoterephthalic acid, 2-hydroxy 4-methoxy benzaldehyde, sodium cyanoborohydride, formic acid, DMF, isopropanol, and various substrates used for catalysis were purchased from commercial sources and used as received.

**Characterization:**  $^1\text{H}$  and  $^{13}\text{C}$  NMR were recorded using a Geol resonance ECZ600R spectrometer at 25 °C. TMS was used as an internal reference during NMR spectroscopic study. Parkin Elmer 883 spectrometer was used to record the FT-IR data using a KBr pellet. The following indications were used to indicate the corresponding absorption bands: very strong (vs), strong (s), medium (m), weak (w), shoulder (sh), and broad (br). JEOL JSM-7100F instrument working at 18 kV accelerating voltage was used to record the FE-SEM data. Before taking the FE-SEM images, the thin coating of Au (~ 4 nm) was coated using a vacuum evaporator. Cu-K $\alpha$  radiation was used to carry out the XRPD study and data was recorded over a  $2\theta$  range of 5-50 °. Thermogravimetric analyses (TGA) were carried out using an SDT Q600 thermogravimetric analyzer in the temperature range of 25-700 °C under an argon atmosphere at a heating rate of 10 °C min<sup>-1</sup>. A Quantachrome Autosorb iQMP gas sorption analyzer was used for the nitrogen sorption experiment at -196 °C.

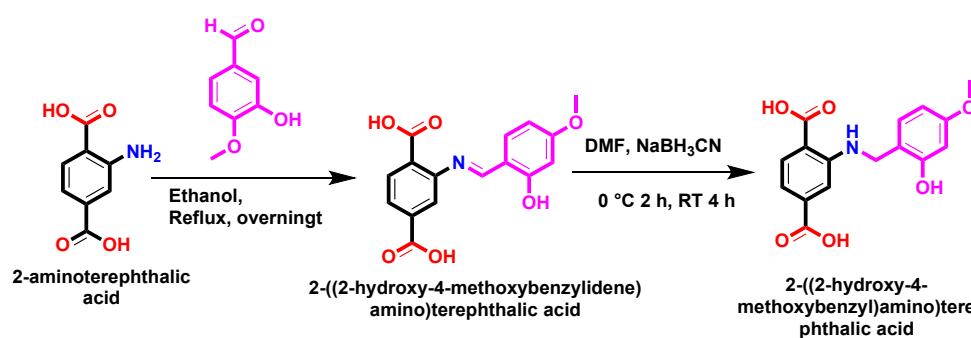
## Synthesis of H<sub>2</sub>BDC-NH-CH<sub>2</sub>-Ph-2OH-4OCH<sub>3</sub> or 2-((2-hydroxy-4-methoxy benzylamino)terephthalic acid):

The below-mentioned synthetic two-step procedures were followed during the synthesis of the 2-((2-hydroxy-4-methoxy benzyl amino) terephthalic acid linker (Scheme S1). In the first step of the synthesis, 2-amino terephthalic acid (4.0 g, 22.0 mmol) was taken in methanol (40 mL) and stirred at 50 °C for 30 min. Afterward, a solution of 2-hydroxy-4-methoxy benzaldehyde (3.6 g, 23.9 mmol) in methanol (20 mL) was gradually added to the previous suspension of 2-amino terephthalic acid. After complete addition, the total reaction mixture was allowed to reflux at 80 °C for 12 h. After 12 h, the yellow product 2-((2-hydroxy-4-methoxy benzylidene)amino) terephthalic acid was filtered and washed with methanol (3×5 mL). Yield: 6.2 g (19.6 mmol, 92%).

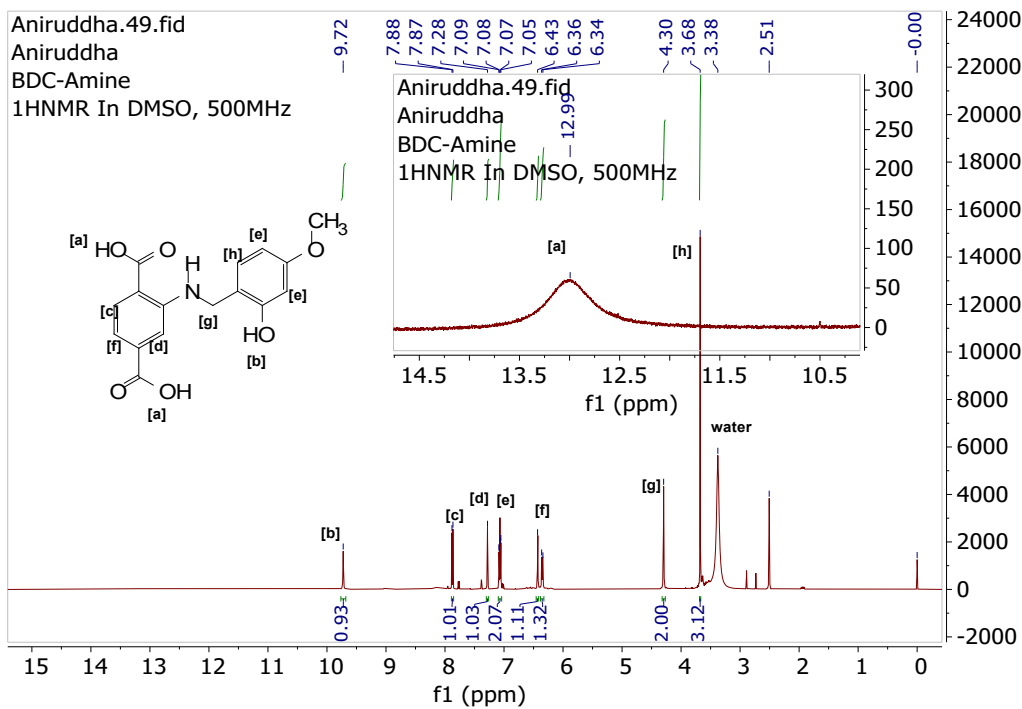
In the second step of the synthesis, the product 2-((2-hydroxy-4-methoxy benzylidene) amino) terephthalic acid (6.2 g, 19.6 mmol) obtained in the previous step was suspended in 50 mL of DMF and stirred at room temperature for 30 min. After that, NaBH<sub>3</sub>CN (1.8 g, 29.4 mmol) was added to the previous suspension at 0 °C and kept under stirring conditions at 0 °C for 2 h. Afterward, the ice bath was removed and the reaction mixture was stirred at room temperature for the next 4 h. After 4 h, the orange color clear reaction mixture was poured onto crushed ice in a beaker and kept for 6 h to achieve complete precipitation of the yellow-colored product. Finally, 2-((2-hydroxy-4-methoxybenzyl) amino) terephthalic acid, the precipitate was collected by vacuum filtration, followed by washing with a sufficient amount of water and drying in a conventional oven at 80 °C for 12 h. Yield: 2.5 g (7.8 mmol, 39%).

<sup>1</sup>H NMR (500 MHz, DMSO-d<sub>6</sub>, δ ppm): 12.99 (2H, br s), 9.72 (1H, s), 7.88 (1H, d), 7.28 (1H, s), 7.07 (2H, t), 6.43 (1H, s), 6.35 (1H, d), 4.30 (2H, s), 3.68 (3H, s).

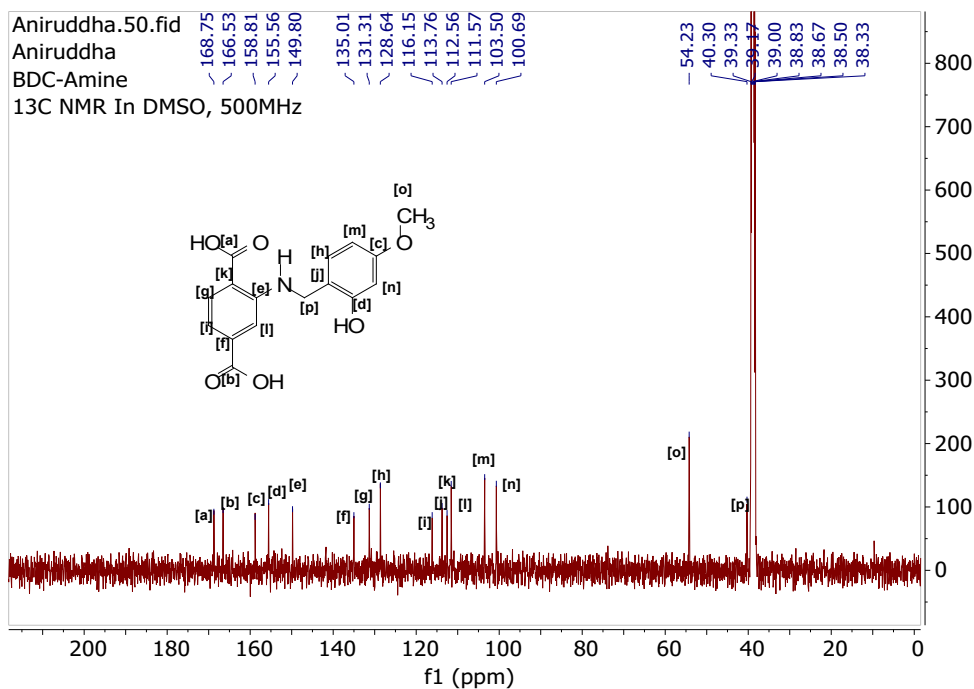
<sup>13</sup>C NMR (125 MHz, DMSO-d<sub>6</sub>, δ ppm): 168.7, 166.5, 158.8, 155.6, 149.8, 135.0, 131.3, 128.6, 116.2, 113.8, 112.6, 111.6, 103.5, 100.7, 54.2, 40.3.



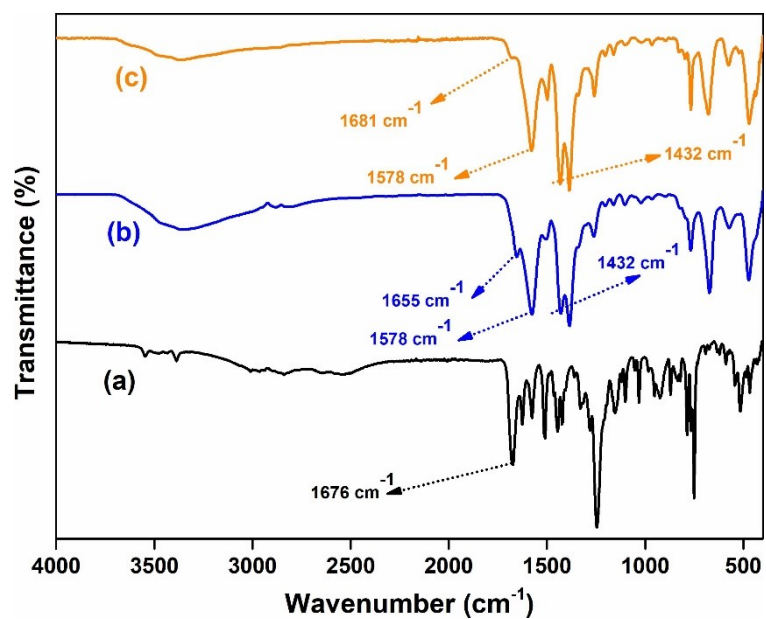
**Scheme S1.** Reaction scheme for the preparation of H<sub>2</sub>BDC-NH-CH<sub>2</sub>-Ph-2OH-4OCH<sub>3</sub> linker.



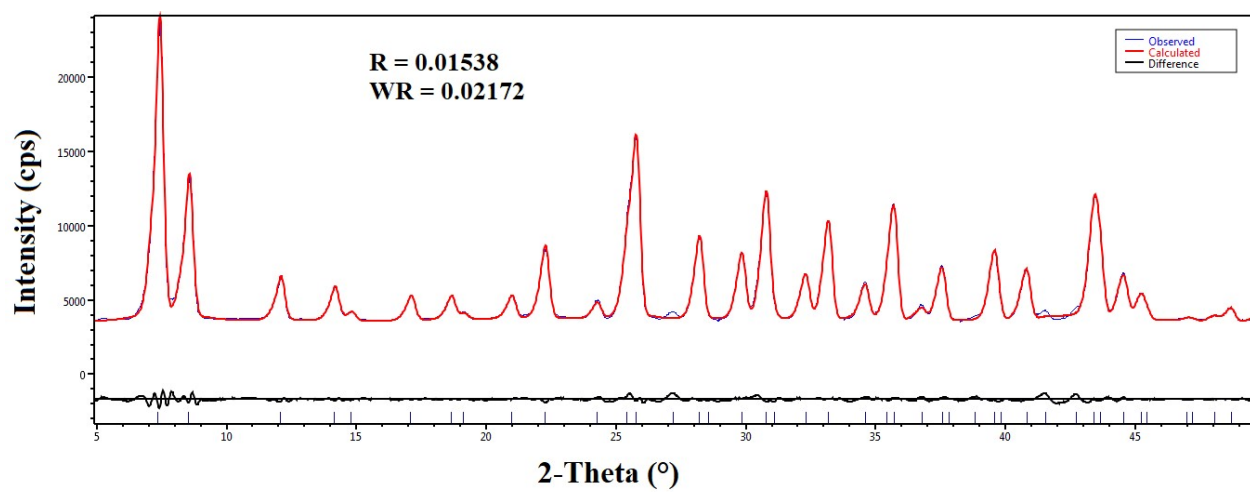
**Fig. S1.** <sup>1</sup>H NMR spectrum of H<sub>2</sub>BDC-NH-CH<sub>2</sub>-Ph-2OH-4OCH<sub>3</sub> linker in DMSO-d<sub>6</sub>.



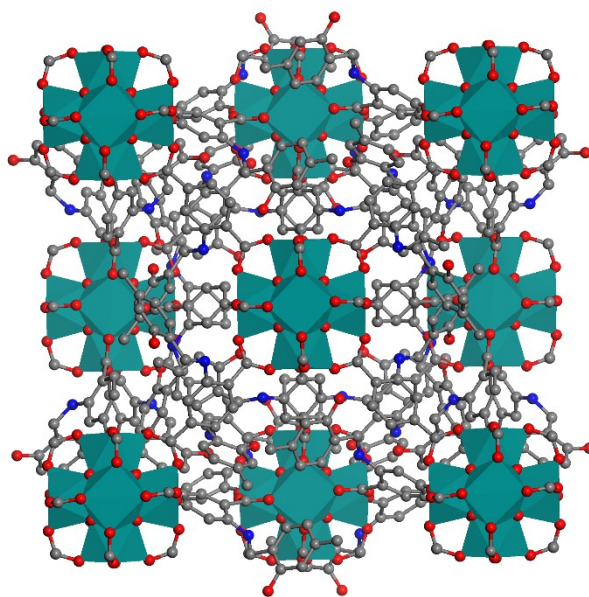
**Fig. S2.** <sup>13</sup>C NMR spectrum of H<sub>2</sub>BDC-NH-CH<sub>2</sub>-Ph-2OH-4OCH<sub>3</sub> linker in DMSO-d<sub>6</sub>.



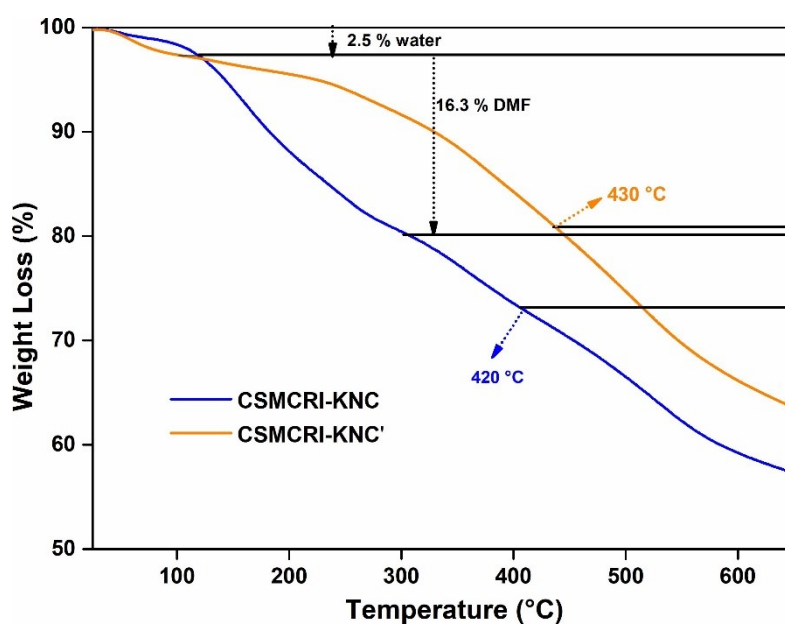
**Fig. S3.** FT-IR spectra of (a)  $\text{H}_2\text{BDC-NH-CH}_2\text{-Ph-2OH-4OCH}_3$  linker (black), (b) as-synthesized CSMCRI-KNC (blue) and (c) CSMCRI-KNC' (orange).



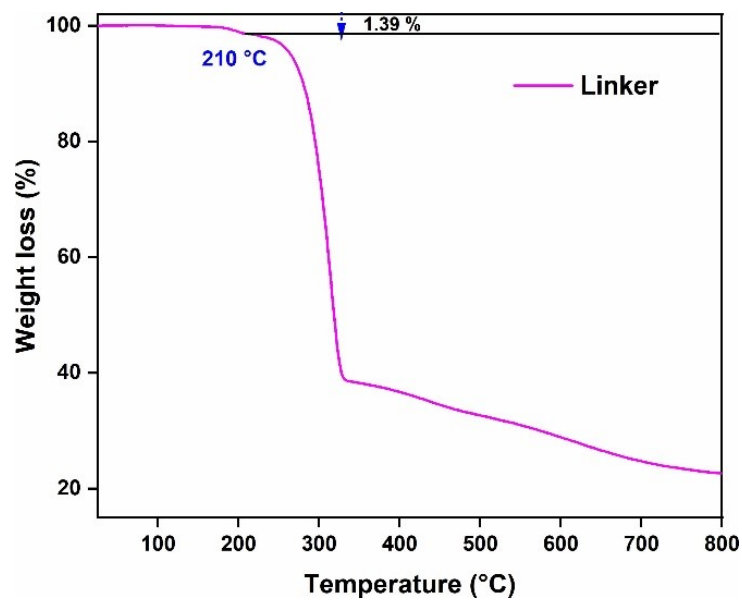
**Fig.S4.** Le Bail fit of the XRPD pattern of MOF CSMCRI-KNC.



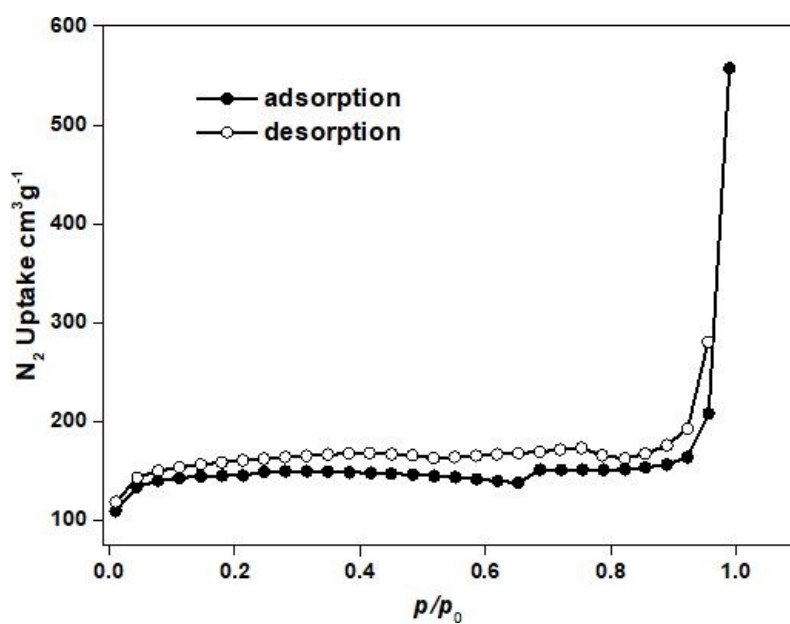
**Fig. S5.** Simulated 3D structural framework of **CSMCRI-KNC** MOF. Colour codes: C, black; O, red; N, blue; Hf, cyanpolyhedra. Hydrogen atoms have been omitted from the phenyl ring of the structural diagram for clarity.



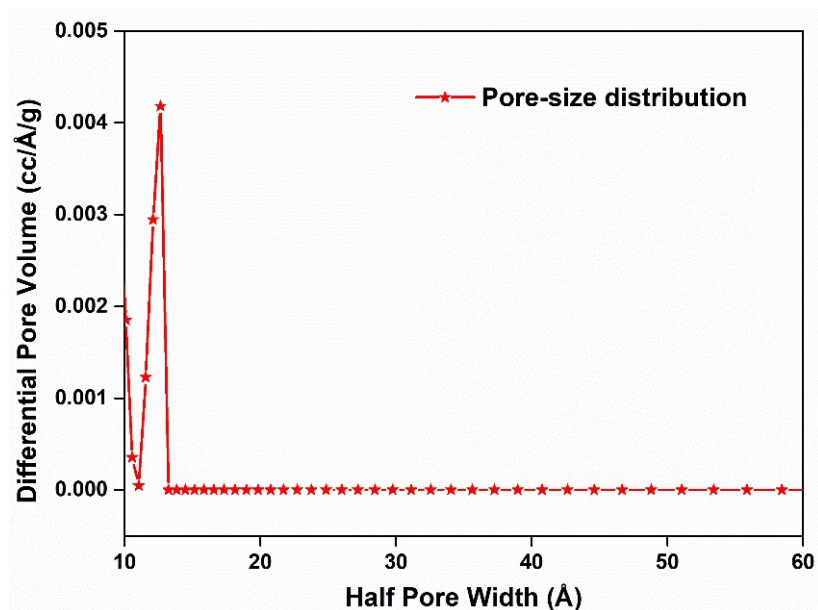
**Fig. S6.** TG curves of as-synthesized **CSMCRI-KNC**(blue) and **CSMCRI-KNC'** (orange) recorded in an  $N_2$  atmosphere in the temperature range of 30-650 °C with a heating rate of 5 °C  $min^{-1}$ .



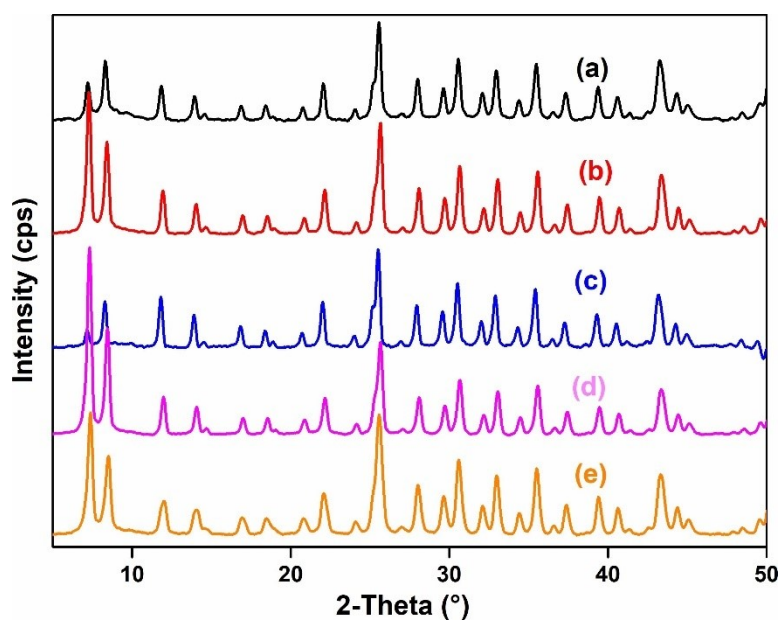
**Fig. S7.** TG curves of linker recorded in an N<sub>2</sub> atmosphere in the temperature range of 30-800 °C with a heating rate of 5 °C min<sup>-1</sup>.



**Fig. S8.** N<sub>2</sub> adsorption (solid circles) and desorption (open circles) isotherms of CSMCRI-KNC' measured at -196 °C.

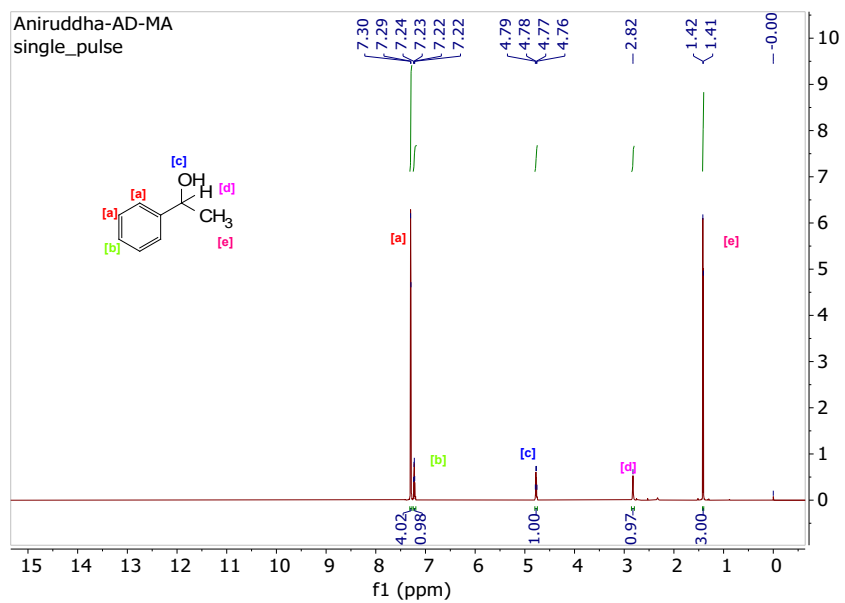


**Fig. S9.** DFT pore-size distribution plot of CSMCRI-KNC' measured at  $-196\text{ }^{\circ}\text{C}$ .

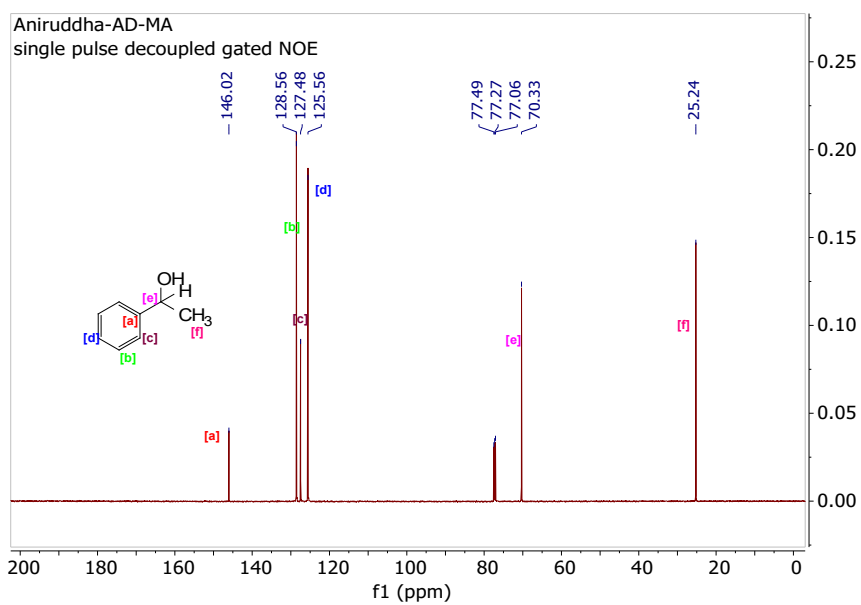


**Fig. S10.** XRPD pattern of CSMCRI-KNC': after stirring in (a) glacial acetic acid, (b) 1,4-dioxane, (c) DMSO, (d) water, and, (e) 1 N HCl for 36 h.

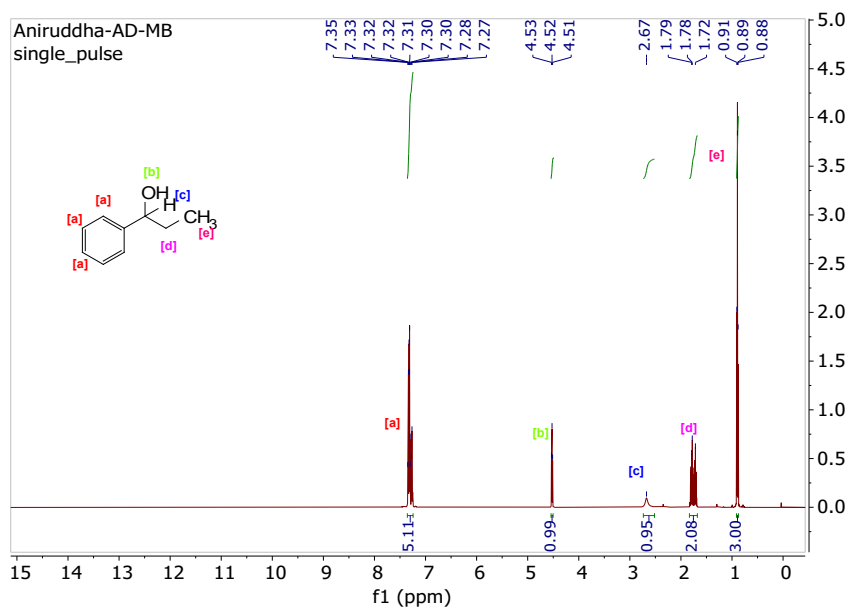




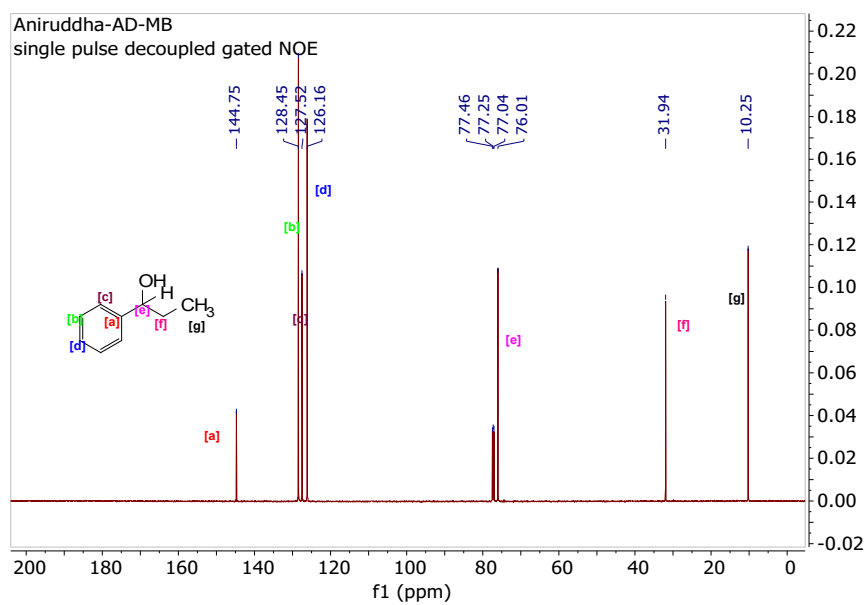
**Fig. S11.** <sup>1</sup>H NMR spectrum of compound **2a** in CDCl<sub>3</sub>.



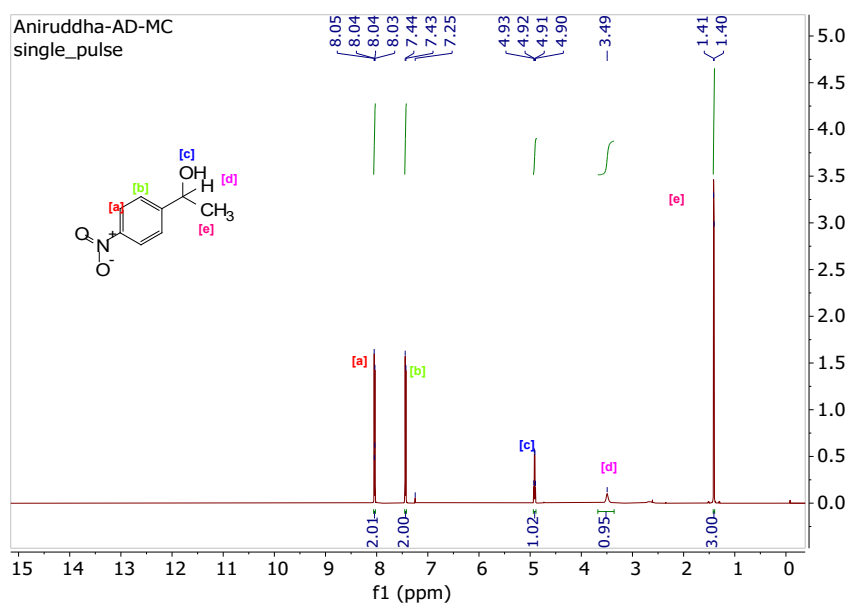
**Fig. S12.** <sup>13</sup>C NMR spectrum of compound **2a** in CDCl<sub>3</sub>.



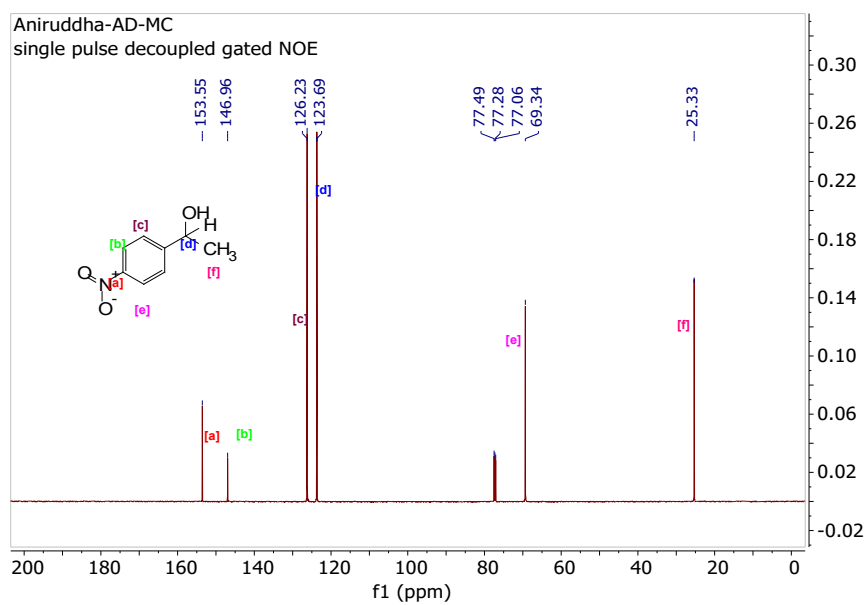
**Fig. S13.**  $^1\text{H}$ NMR spectrum of compound **2b** in  $\text{CDCl}_3$ .



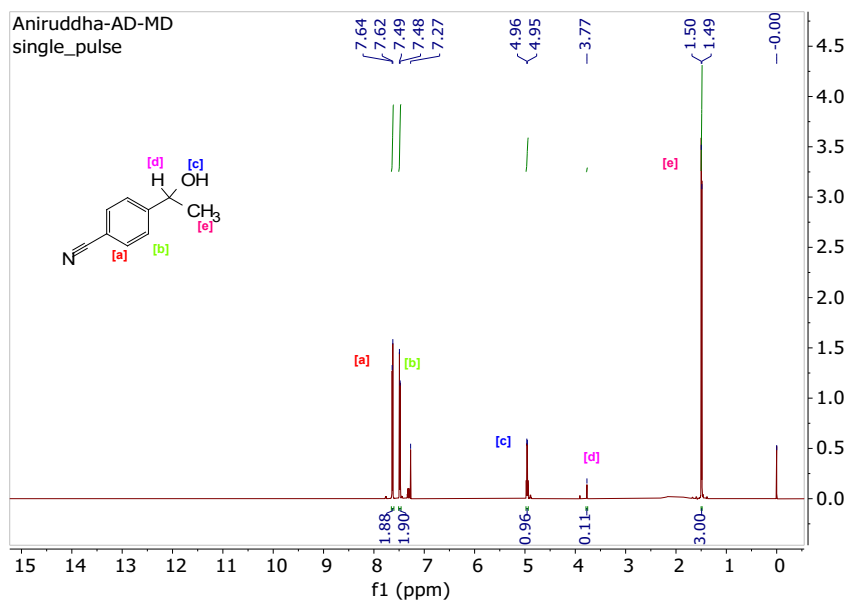
**Fig. S14.**  $^{13}\text{C}$ NMR spectrum of compound **2b** in  $\text{CDCl}_3$ .



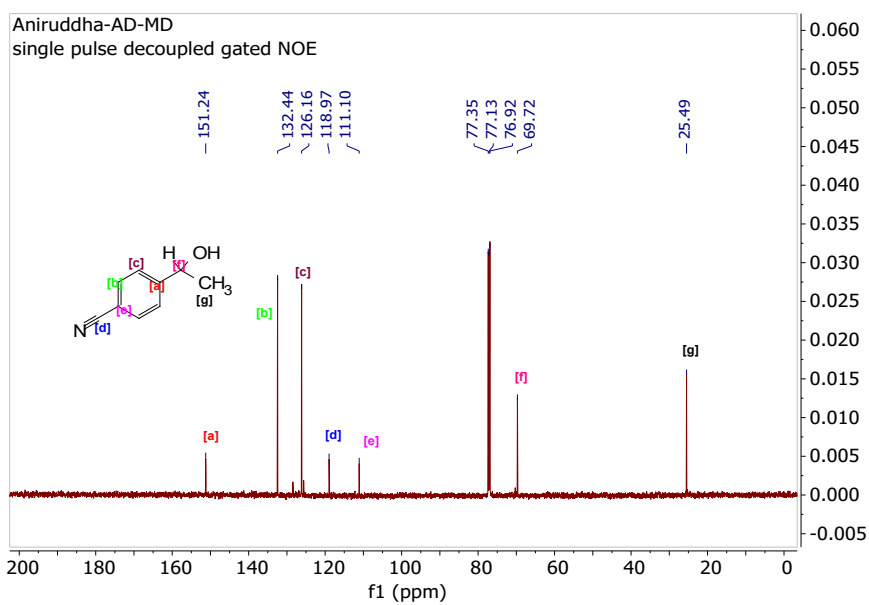
**Fig. S15.**  $^1\text{H}$ NMR spectrum of compound **2c** in  $\text{CDCl}_3$ .



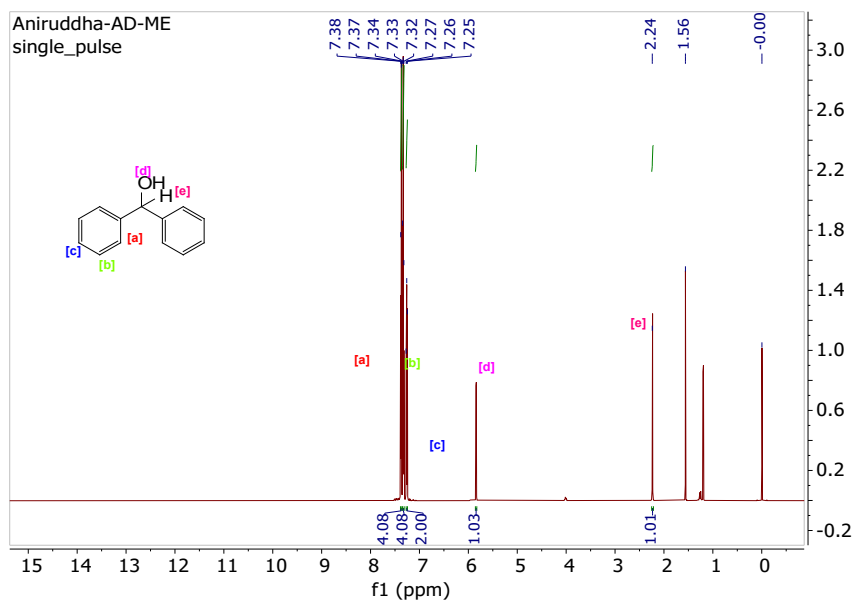
**Fig. S16.**  $^{13}\text{C}$ NMR spectrum of compound **2c** in  $\text{CDCl}_3$ .



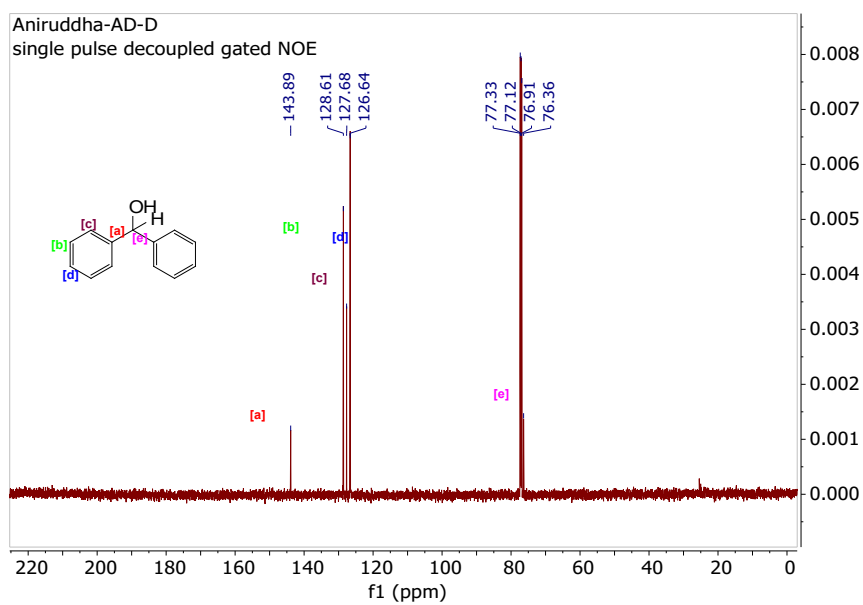
**Fig. S17.**  $^1\text{H}$ NMR spectrum of compound **2d** in  $\text{CDCl}_3$ .



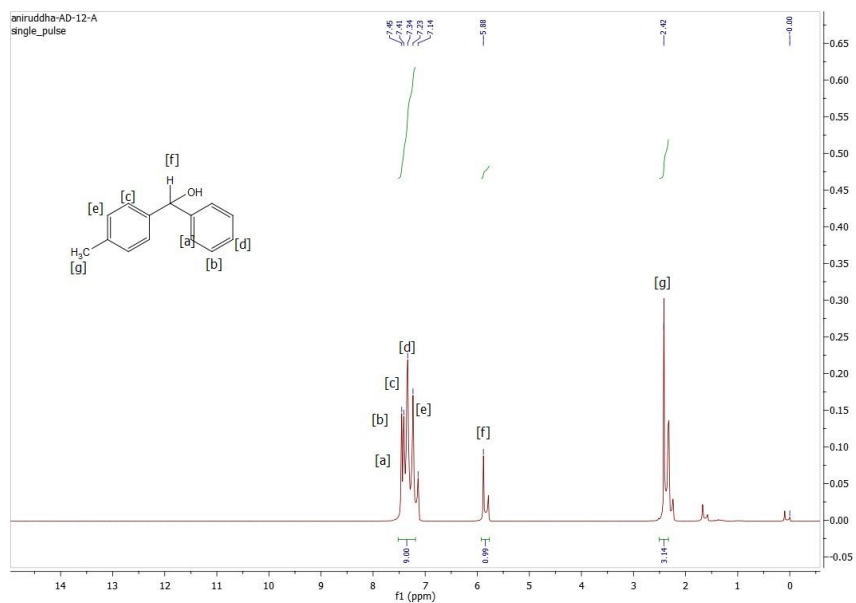
**Fig. S18.**  $^{13}\text{C}$ NMR spectrum of compound **2d** in  $\text{CDCl}_3$ .



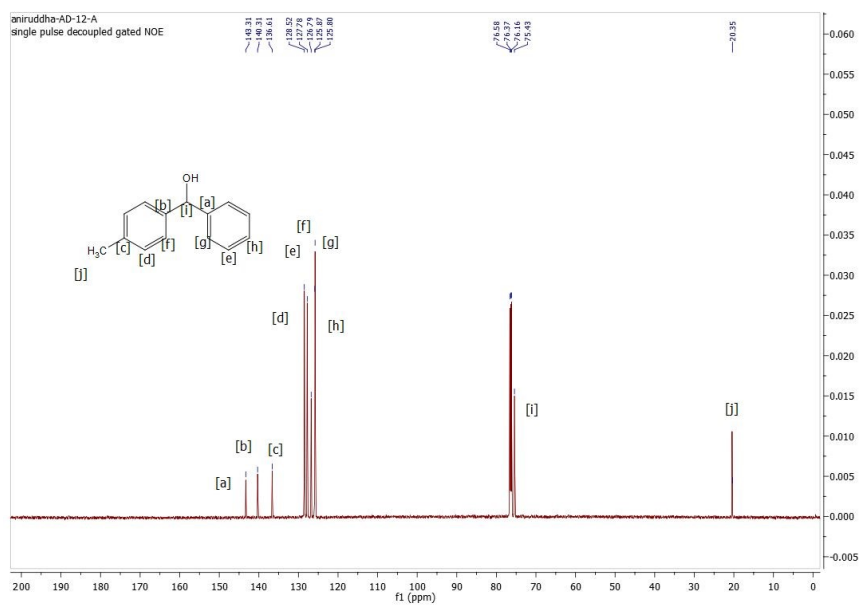
**Fig. S19.**  $^1\text{H}$ NMR spectrum of compound **2e** in  $\text{CDCl}_3$ .



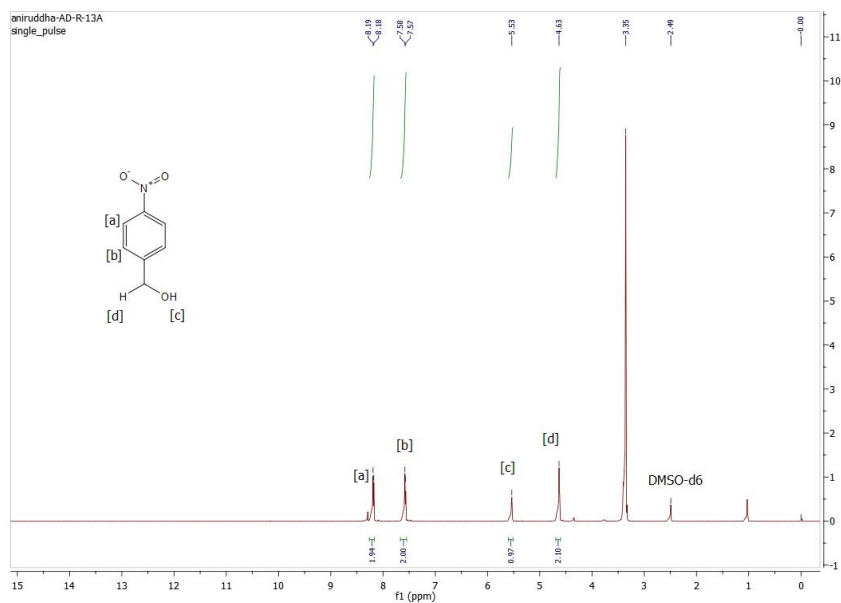
**Fig. S20.**  $^{13}\text{C}$ NMR spectrum of compound **2e** in  $\text{CDCl}_3$ .



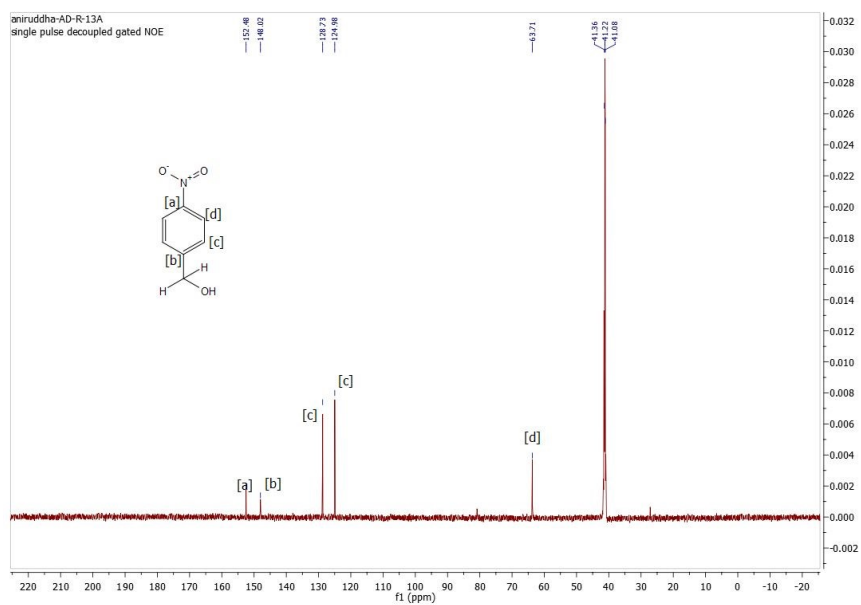
**Fig. S21.**  $^1\text{H}$ NMR spectrum of compound **2f** in  $\text{CDCl}_3$ .



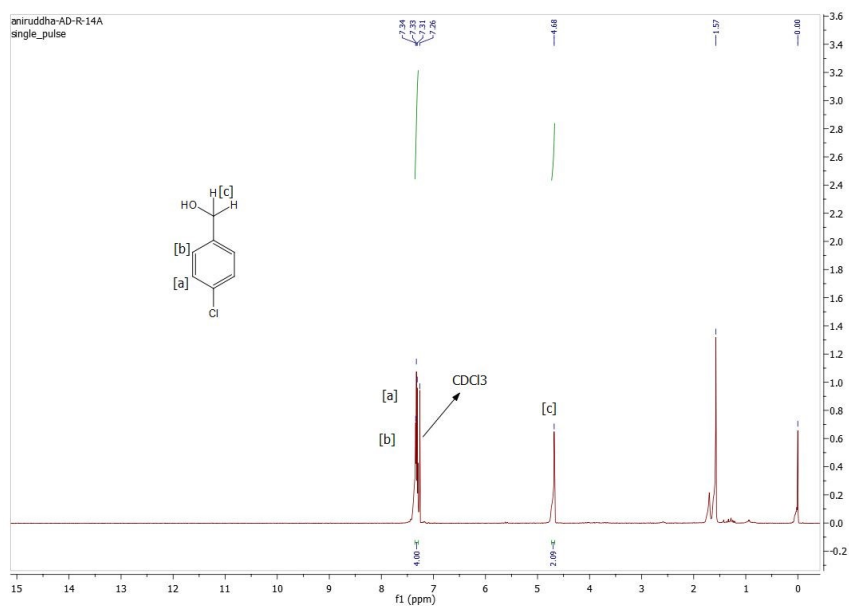
**Fig. S22.**  $^{13}\text{C}$ NMR spectrum of compound **2f** in  $\text{CDCl}_3$ .



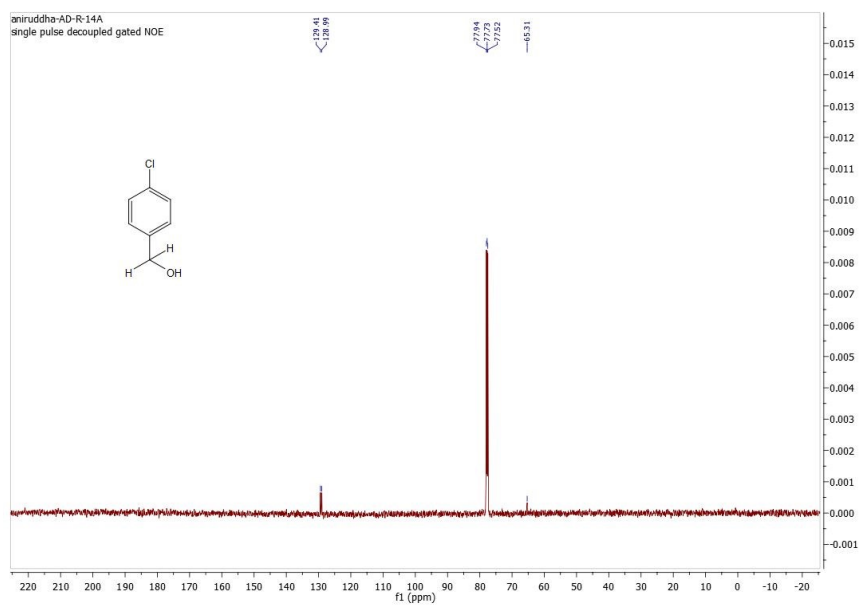
**Fig. S23.**  $^1\text{H}$ NMR spectrum of compound **2g** in  $\text{DMSO-d}_6$ .



**Fig. S24.**  $^{13}\text{C}$ NMR spectrum of compound **2g** in  $\text{CDCl}_3$ .

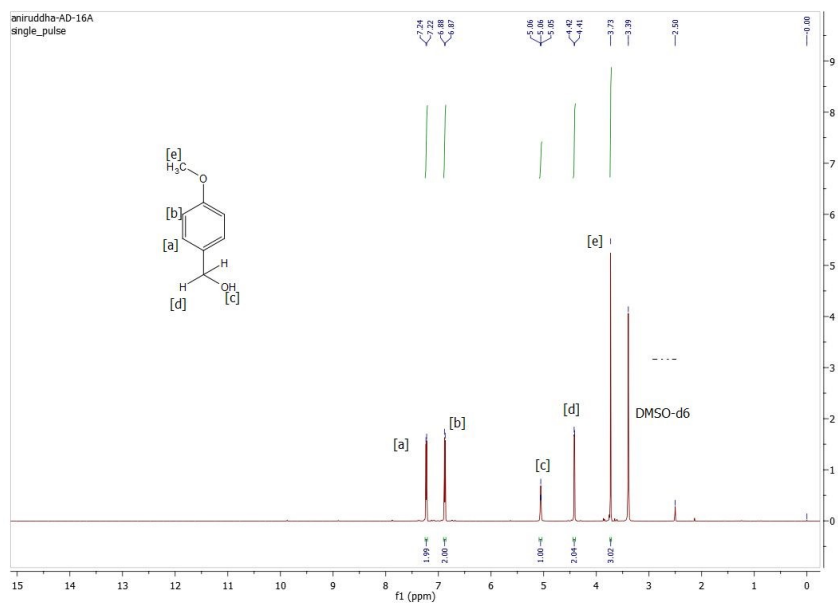


**Fig. S25.** <sup>1</sup>H NMR spectrum of compound **2h** in CDCl<sub>3</sub>.

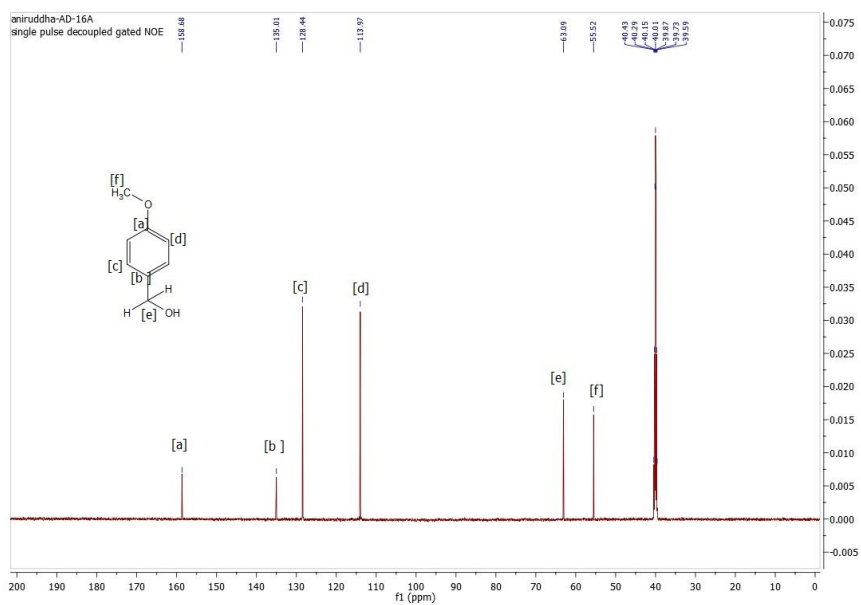


**Fig. S26.** <sup>13</sup>C NMR spectrum of compound **2h** in CDCl<sub>3</sub>.

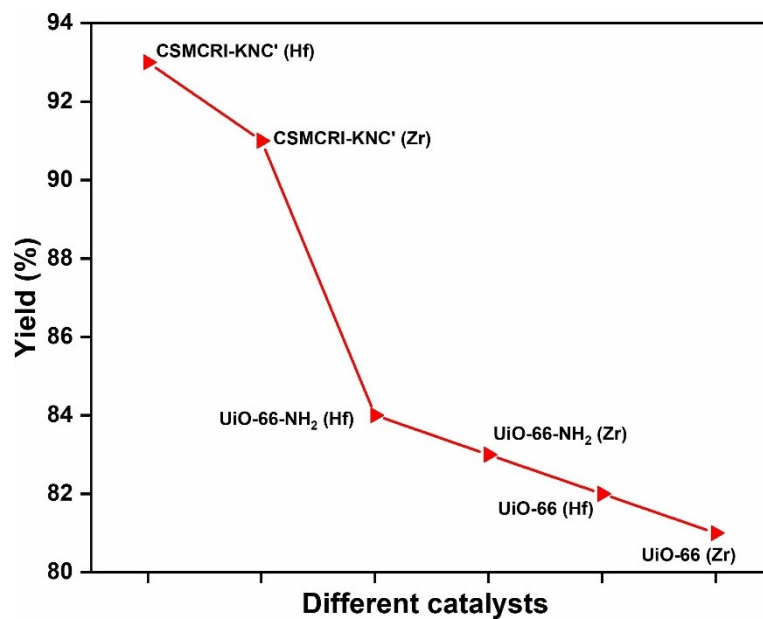




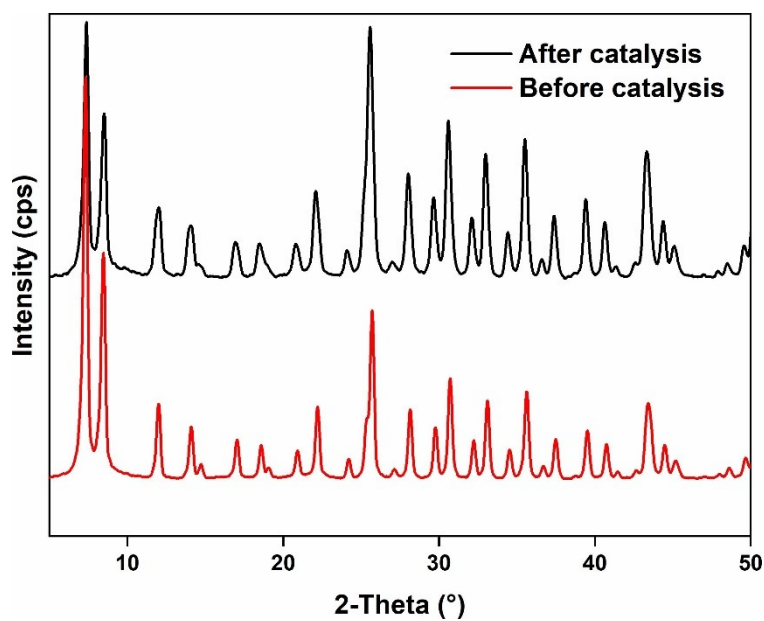
**Fig. S27.** <sup>1</sup>H NMR spectrum of compound **2i** in DMSO-d<sub>6</sub>.



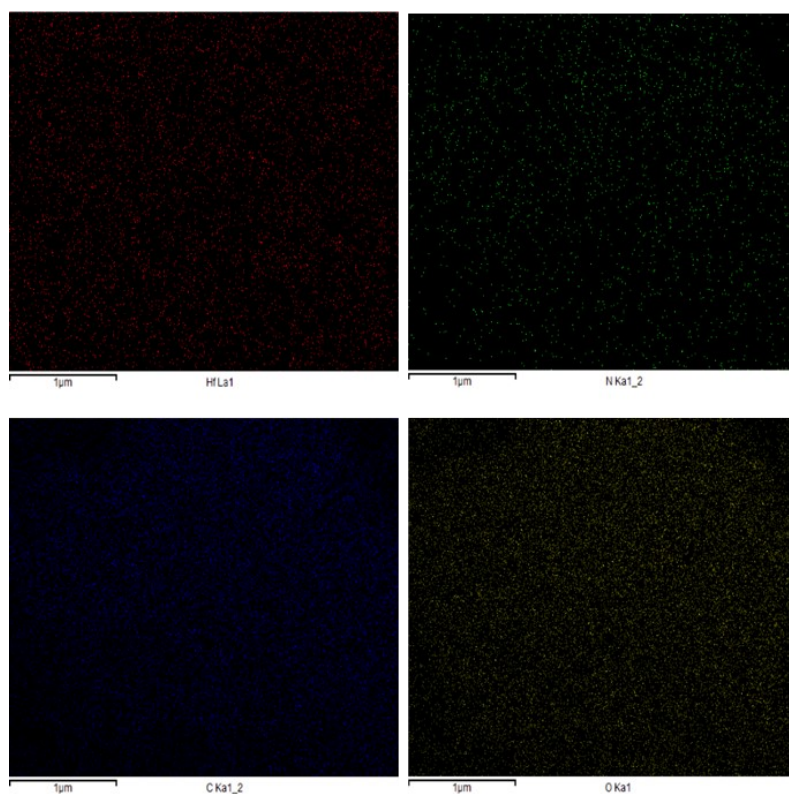
**Fig. S28.** <sup>13</sup>C NMR spectrum of compound **2i** in CDCl<sub>3</sub>.



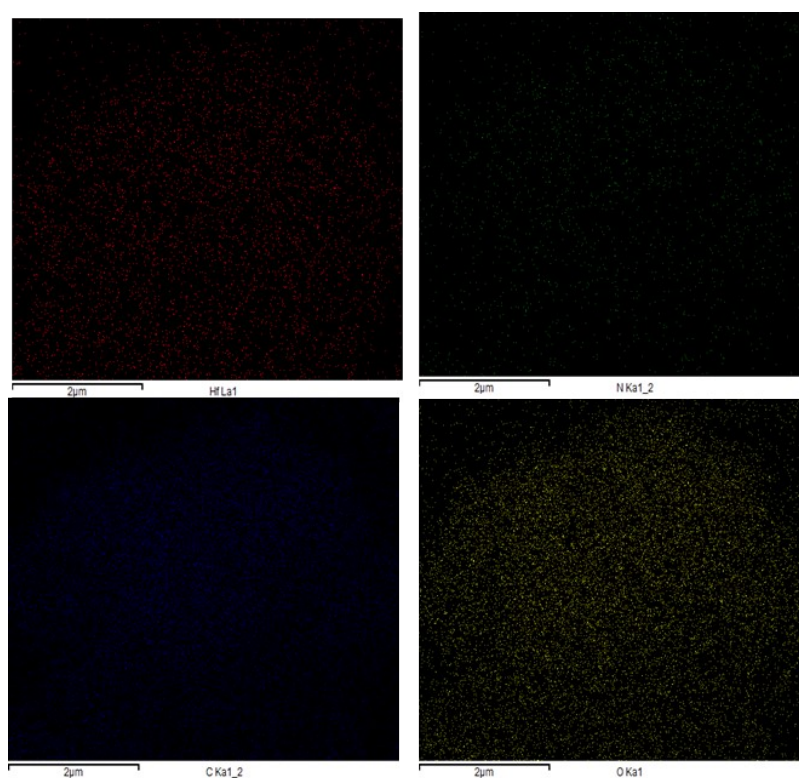
**Fig. 29.** The yield (%) obtained on the MPV reduction of acetophenone using different UiO-66 MOFs as catalysts under the given reaction conditions.



**Fig. S30.** XRPD pattern of CSMCRI-KNC': before (red) and after (black) catalysis.



**Fig. S31.** EDX elemental mapping of CSMCRI-KNC' before catalysis.

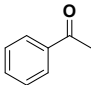
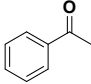
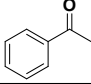
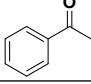
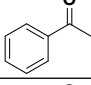
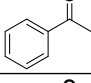
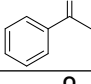
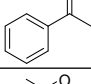
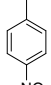
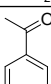


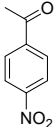
**Fig. S32.** EDX elemental mapping of CSMCRI-KNC' after catalysis.

**Table S1.** Unit cell parameters of as-synthesized CSMCRI-KNC obtained by indexing its XRPD pattern. The obtained values were compared with those of the previously reported unfunctionalized and functionalized UiO-66 MOFs.

Entry	Name of the MOF	Cell length (a = b = c)	Cell angle ( $\alpha = \beta = \gamma$ )	Crystal system	V ( $\text{\AA}^3$ )	References
1	CSMCRI-KNC	20.7078(6)	90.000	Cubic	8879.8(4)	This work
2	Zr-UiO-66	20.7004(2)	90.000	Cubic	8870.3(2)	1
3	Zr-UiO-66-NH-CH <sub>2</sub> -Py	20.755(3)	90.000	Cubic	8940.3(21)	2

**Table S2.** Comparative catalytic performances between various Hf-based UiO-66 MOFs/other MOF based heterogeneous catalysts where the main structural topology of catalysts/substrates are same.

Entry	Name of Compound	Substrate Used	Yield (%)	Temperature (°C)	Time (h)	References
1	CSMCRI-KNC'(Hf)		93	140	8	This work
2	CSMCRI-KNC'(Zr)		91	140	8	This work
3	UiO-66-NH <sub>2</sub> (Hf)		84	140	8	This work
4	UiO-66-NH <sub>2</sub> (Zr)		83	140	8	This work
5	UiO-66 (Hf)		82	140	8	This work
6	UiO-66 (Zr)		81	140	8	This work
7	M-MOF-808		92.5	82	8	3
8	Zr-MTT		98.1	150	12	4
9	Hf-MOF-808		99	120	3	5
10	Hf-UiO-66-(OH) <sub>2</sub>		96	120	3	5

11	Zr-BDB		96.2	150	10	6
----	--------	---	------	-----	----	---

### References.

1. J. H. Cavka, S. Jakobsen, U. Olsbye, N. Guillou, C. Lamberti, S. Bordiga and K. P. Lillerud, *J. Am. Chem. Soc.*, 2008, **130**, 13850–13851.
2. A. Das, N. Anbu, M. SK, A. Dhakshinamoorthy and S. Biswas, *Dalton Trans.*, 2019, **48**, 17371-17380.
3. A. H. Valekar, M. Lee, J. W. Yoon, J. Kwak, D.-Y. Hong, K.-R. Oh, G.-Y. Cha, Y.-U. Kwon, J. Jung, J.-S. Chang and Y. K. Hwang, *ACS Catal.*, 2020, **10**, 3720–3732.
4. J. Song, C. Xie, Z. Xue and T. Wang, *ACS Sustainable Chem. Eng.*, 2022, **10**, 12197–12206.
5. Y. Lin, Q. Bu, J. Xu, X. Liu, X. Zhang, G.-P. Lu and B. Zhou, *Molecular Catalysis*, 2021, **502**, 111405-111411.
6. J. Song, M. Hua, X. Huang, A. Visa, T. Wu, H. Fan, M. Hou, Z. Zhang and B. Han, *Green Chem.*, 2021, **23**, 1259–1265.